

$\text{Fe}_3\text{O}_4@\text{SiO}_2\text{-NH}_2$ as an efficient nanomagnetic carrier for controlled loading and release of acyclovir

Reza Tayebee^{1*}; Mojtaba Fattahi Abdizadeh^{2*}; Mostafa Mohammadpour Amini³;
Nasrin Mollania⁴; Zahra Jalilli¹, Hamed Akbarzadeh⁴

¹Department of Chemistry, School of Sciences, Hakim Sabzevari University, Sabzevar, Iran

²Cellular and Molecular Research Center, Sabzevar University of Medical Sciences, Sabzevar, Iran

³Department of Chemistry, Shahid Beheshti University, Tehran, Iran

⁴Department of Biology, School of Sciences, Hakim Sabzevari University, Sabzevar, Iran

Received 27 June 2017; revised 24 August 2017; accepted 07 September 2017; available online 11 September 2017

Abstract

Considering many applications of functionalized metal oxide nanoparticles in magnetic resonance imaging, drug delivery, neutron irradiation, electronics, catalysis and optics; herein, a new strategy is developed to functionalize magnetite nanoparticles to improve their performances in the delivery of acyclovir. In this study, magnetite Fe_3O_4 nanoparticles are synthesized by hydrothermal method. Then, the surface hydroxyl groups were extended by treating with TEOS (tetraethyl orthosilicate); Finally, TPA (trimethoxysilylpropylamine) was anchored to the surface hydroxyl groups to produce amino-functionalized $\text{Fe}_3\text{O}_4@\text{SiO}_2\text{-NH}_2$ magnetic nanoparticles. The synthesized sample was characterized by UV-Vis, FESEM, FT-IR, and XRD. Afterward, the functionalized nanoparticles were examined in the delivery of acyclovir as an active antiviral drug model involving amine and hydroxyl functional groups. For this purpose, the amount of loading/release of the drug was investigated in different pHs, including mouth and stomach pH values. The screened experimental parameters in this study revealed that the prepared magnetite nanoparticles decorated with amine functional groups are successful in the controlled delivery of acyclovir.

Keywords: Amine functionalized; Acyclovir; Drug delivery; Magnetite; Silica; XRD.

How to cite this article

Tayebee R, Fattahi Abdizadeh M, Amini M M, Mollania N, Jalilli Z. $\text{Fe}_3\text{O}_4@\text{SiO}_2\text{-NH}_2$ as an efficient nanomagnetic carrier for controlled loading and release of acyclovir. *Int. J. Nano Dimens.*, 2017; 8 (4): 367-372.

INTRODUCTION

During the past twenty years, nanoparticles have been regularly carried out in controlled clinical human sciences [1]. Thereafter, a wide range of research in nanoscale therapeutic and diagnostic agents have been ascended in the domain of biomedical nanotechnologies [2–4], protein–drug nanoconjugates [5], micelles [6], liposomes [7] dendrimers [8], inorganic nanoparticles [9] and other drug nanoconjugates [10]. Recently, many attempts have been carried out to design and synthesize new targeted biocompatible compounds with a high capacity for loading and controlled release of desired drug molecules which can show minimum leakage of the drug molecules before reaching the target

organ. A number of biocompatible carrier systems involving large surface areas and tailorable pore size are introduced for drug delivery, such as calcium phosphate cement [11], organic polymers [12], various inorganic composites [13], metal-organic frameworks [14] and nanoporous silica [15,16]. Inevitably, the release rate of drugs can be affected by important parameters such as pores size and functional groups anchored to the surface of the carrier [17]. The surface modification could be effective [18] and makes the pores full of the desired functional groups, which can interact with drugs and control drug delivery processes [19]. Magnetic iron oxide nanoparticles bearing relatively large surface area and have been known as potential carriers in drug delivery with multiple practical applications in medicine and biology

* Corresponding Author Email: rtayebee@hsu.ac.ir
mjtabafattahi@gmail.com

due to their multifunctional properties, super paramagnetism and low toxicity [20-22].

Post-synthetic grafting of silanol groups is used as an impressive method to modify the surface, particularly external surface of magnetite nanoparticles. In this way, the fabricated well ordered mesoporous Fe_3O_4 nanomaterial interacts with organosilane in anhydrous toluene under reflux to impel a thin layer of silanol groups around the magnetite nanoparticles. Then, the organic functionalities can essentially be found outside the surface nearby the pore cavities of the ordered pore structure and Fe_3O_4 nanoparticles with uniform morphology will be attaining (Fig. 1).

The purpose of this investigation is constructing of a well ordered magnetic core/mesoporous shell $\text{Fe}_3\text{O}_4@ \text{SiO}_2$ spheres and surface modification of the prepared nanomaterial with trimethoxysilyl propylamine. Then, the fabricated nanocarrier was used for the promising delivery of acyclovir as a model antiviral drug. Influences of the type and concentration of the surfactant, pH, contact time and temperature on the loading/release of acyclovir, loading capacity, and in vitro potential for drug adsorption enhancement of $\text{Fe}_3\text{O}_4@ \text{SiO}_2$ -

NH_2 are systematically investigated.

EXPERIMENTAL

Methods and Materials

All chemicals were received from commercial resources (Merck and Aldrich) and utilized without further refinement. Field emission scanning electron microscope (FESEM) micrographs were taken by applying a KYKY-EM3200 microscope (acceleration speed voltage 26 kV). FT-IR spectra were recorded on an 8700 Shimadzu Fourier Transform Spectrophotometer in the range of 400 to 4000 cm^{-1} utilizing KBr pellets. The crystalline structure of the samples were assessed by X-ray diffraction (XRD) analysis on a PW1800-PHILIPS diffractometer with $\text{Cu K}\alpha$ radiation ($\lambda = 1.5418 \text{ \AA}$) at 40 keV and 40 mA. UV-Vis spectra were recorded on a photonics-Ar-2015 with Ava Lamp DH-S Setup in 200-700 nm rang. A freeze dryer, Model FD-10, Pishtaz Equipment Engineering Co, Iran, was applied for drying of the prepared nanomaterials. Fe_3O_4 and $\text{Fe}_3\text{O}_4@ \text{SiO}_2\text{-NH}_2$ core-shell nanoparticles were synthesized by the introduced single step solvothermal method with a few modifications [23-24].

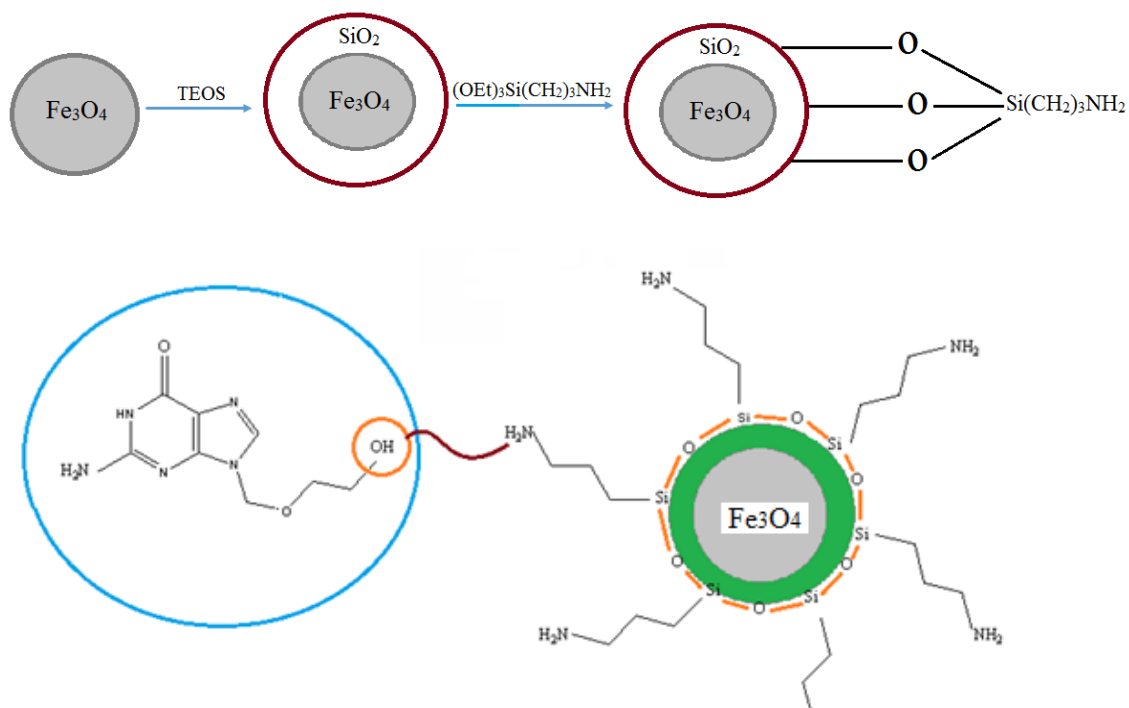


Fig. 1: General route for the synthesis and interaction of $\text{Fe}_3\text{O}_4@ \text{SiO}_2\text{-NH}_2$ with acyclovir.

Preparation of Fe_3O_4 nanoparticles by solvothermal method

Fe_3O_4 nanoparticles were prepared similar to the reported typical synthetic procedure. $FeCl_3 \cdot 6H_2O$ (1.8 g), $NaNO_3 \cdot 3H_2O$ (0.36 g), PEG-400 (45 ml) and 5 ml ethanol were mixed under intense stirring at room temperature for 30 min. Then, 2 g of NaAc was added and the resulting suspension was mixed under intense stirring at room temperature for 12 h. After that, the mixture was put on a Teflon-lined stainless steel autoclave of 50 ml volume. Eventually, the autoclave was warmed and retained at 200 °C for 10 h, afterward chilled off to 25 °C. The dark particles were washed a few times with absolute ethanol and were dried by a rotary evaporator [23].

Preparation of silica-coated $Fe_3O_4@SiO_2$ via surface modification with TEOS

A one-step synthesis was used to obtain silica-coated Fe_3O_4 nanoparticles. 0.1 g of Fe_3O_4 was dispersed in a mixture containing distilled water (2 ml), absolute ethanol (6 ml) and ammonia (0.2 ml, 25%) under sonication for 30 min. Then, the reaction mixture was conducted with 0.5 ml TEOS and was stirred for 16 h. Then, the black precipitate was filtered by an external magnet and well dried.

Surface modification of $Fe_3O_4@SiO_2$ by grafting of TMPA (trimethoxysilyl propylamine)

$Fe_3O_4@SiO_2$ (0.04 g) was spread out in 1.6 ml of dry toluene by ultrasonication for 30 min under N_2 . Then, 0.04 ml of TMPA was joined and the resulting suspension was refluxed under nitrogen for 24 h. After completion of the reaction, the resulting $Fe_3O_4@SiO_2-NH_2$ was isolated by filtration, washed with acetone and dried at room temperature.

Loading and release studies

The drug loading was studied by adding $Fe_3O_4@SiO_2-NH_2$ nanoparticles (0.02 g) into a phosphate buffer (2 ml, pH 7.4) containing acyclovir (2 mg) with magnetic stirring at 55 °C for 5 h. Then, the mixture was isolated via an external magnet and the supernatant was utilized for measuring the drug loading amount. To delete the unloaded acyclovir, the precipitate was re-dispersed in 2 ml of the above buffer and washed until the filtrate was clear. The free-acyclovir content in the supernatant was quantified by UV-Vis at 253 nm. Amount of the loaded drug was calculated by Eq. (1) [25].

$$\text{Loading content} = \frac{M_0 - M_t}{M_N} \times 100 \% \quad \text{Eq. (1)}$$

Where, M_0 and M_t are the amounts of acyclovir in the primary and filtered solutions, respectively. M_N is the amount of $Fe_3O_4@SiO_2-NH_2$ used for the loading process.

The in vitro release of acyclovir from $Fe_3O_4@SiO_2-NH_2$ was screened through the dialysis method. To release of the loaded acyclovir, 2 mg of acyclovir-loaded nanoparticles $Fe_3O_4@SiO_2-NH_2$ were put into a dialysis bag; then, the bag was located in a solution containing 2 ml of phosphate buffer and 3 ml of deionized water. Finally, the bag was immersed in the solutions at 55 °C. The released acyclovir out of the dialysis bag was sampled at a determined period and measured by UV-Vis at 253 nm. To determine the amount of the drug adsorbed after 1, 2, 4, 8, 24 and 48 h, 1 ml of the above solution was replaced with a fresh buffer solution and was analyzed by UV-Vis [26]. Loading process would be achieved via the hydrogen bonding interactions of the hydroxyl groups of acyclovir with the surface amino groups of $Fe_3O_4@SiO_2-NH_2$. To study impact of drying conditions on the loading efficacy of the modified nanomaterial, the prepared final compound was dried under freeze conditions. Results showed only a little enhancement in the loading capacity compared with the one dried under usual thermal conditions.

RESULTS AND DISCUSSION

Characterization of $Fe_3O_4@SiO_2-NH_2$

Since, acyclovir and a large number of antiviral drugs cause various allergenic side effects; therefore, designing new biocompatible drug carrier systems bearing less harmful impacts for oral delivery is necessary. The present new modified nanomaterial has a number of benefits such as being biocompatible, extended surface area and uniform pore size which permit drug molecules to be adsorbed easily. Moreover, $Fe_3O_4@SiO_2-NH_2$ showed good dispersibility in the aqueous solutions.

Fig. 2 shows the FT-IR spectra of acyclovir, $Fe_3O_4@SiO_2-NH_2$, and acyclovir loaded $Fe_3O_4@SiO_2-NH_2$. The reaction of hydroxyl groups on the surface of $Fe_3O_4@SiO_2$ with the ethoxy groups of trimethoxysilylpropylamine ended to the formation of a novel carrier system. Presence of bands at almost 622, 900 and 1050 cm^{-1} are attributed to the Fe-O, Si-O-H and Si-O-Si vibrations, respectively. The presence of C-H

bending and stretching vibrations about 1600 and 2850 cm^{-1} , respectively, in the FT-IR of $\text{Fe}_3\text{O}_4@ \text{SiO}_2\text{-NH}_2$ clearly confirmed that propylamine groups are successfully grafted on the surface of the nanomagnetic material. The bands at 3355 and 2920 cm^{-1} in the FT-IR spectrum were ascribed to N–H and C–H stretching vibrations and corroborated that the amine groups are joined to the surface of nanomagnetic material. The grafted amine groups at the surface of $\text{Fe}_3\text{O}_4@ \text{SiO}_2\text{-NH}_2$ provided hydrogen bond interactions with the oxygen atoms of acyclovir and caused immobilization of the drug molecules onto the carrier surface [27–28].

According to the chemical structure of acyclovir, the presence of C=O stretching vibration at 1701 cm^{-1} , together with aliphatic C–H stretching vibrations in 2940–2960 cm^{-1} for the alkyl groups and N–H stretching vibrations in 3280–3335 cm^{-1} unambiguously confirmed loading of the acyclovir. Moreover, the bands at 1090, 1420, and 1550 cm^{-1} are assigned to C–N, C–H, and N–H bending vibrations, respectively.

The XRD patterns for Fe_3O_4 and drug loaded $\text{Fe}_3\text{O}_4@ \text{SiO}_2\text{-NH}_2$ are depicted in Fig. 3. It is assigned

that the relative intensities and positions of the reflection peaks for Fe_3O_4 nanoparticles agree well with the standard diffraction card JCPDS 12882–54552. Comparing the XRD pattern of initial Fe_3O_4 nanoparticles to the modified one displayed that the pores remained intact after functionalization (Fig. 3) [29]. The attendance of a distinct peak at nearly $2\theta = 35$, that matches with the reported ones, authenticated that the pores retained after functionalization and the structure of magnetite remained intact after drug loading.

Size and morphology of Fe_3O_4 and $\text{Fe}_3\text{O}_4@ \text{SiO}_2\text{-NH}_2$ were further studied with FESEM. Fig. 4 describes that Fe_3O_4 nanoparticles were semi-spherical in shape; therefore, the prepared Fe_3O_4 nanoparticles by solvothermal method resulted in uniform sizes with good dispersibility. The average grain size obtained by XRD via the Scherrer equation for Fe_3O_4 (< 25 nm) were in good agreement with the results obtained by FESEM. The FESEM images for $\text{Fe}_3\text{O}_4@ \text{SiO}_2\text{-NH}_2$ nanoparticles before and after drug loading confirmed that the semi-spherical shape of the nanoparticles was unchanged and no observable change in morphology of the nanoparticles occurred.

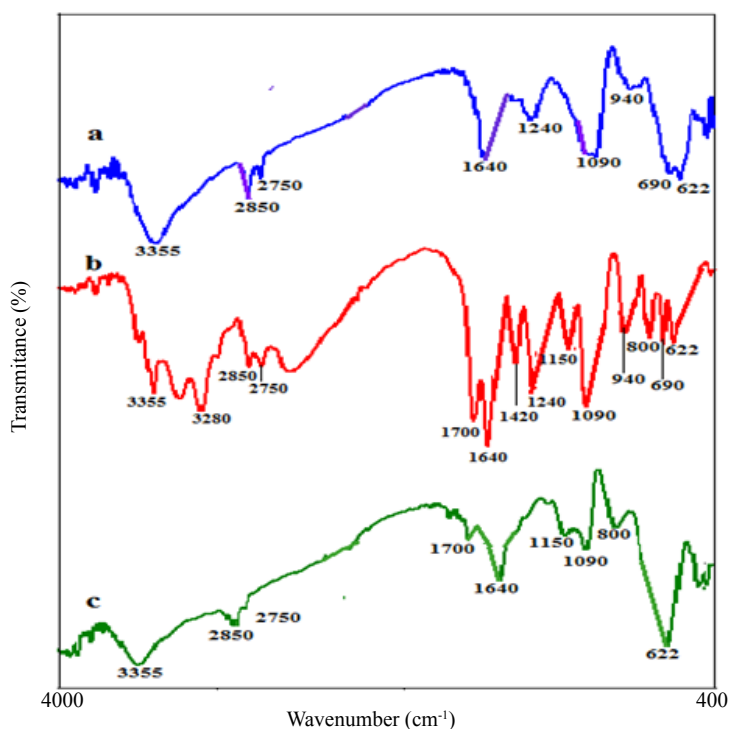


Fig. 2: FT-IR spectra of acyclovir (a), $\text{Fe}_3\text{O}_4@ \text{SiO}_2\text{-NH}_2$ (b), and drug loaded $\text{Fe}_3\text{O}_4@ \text{SiO}_2\text{-NH}_2$ (c).

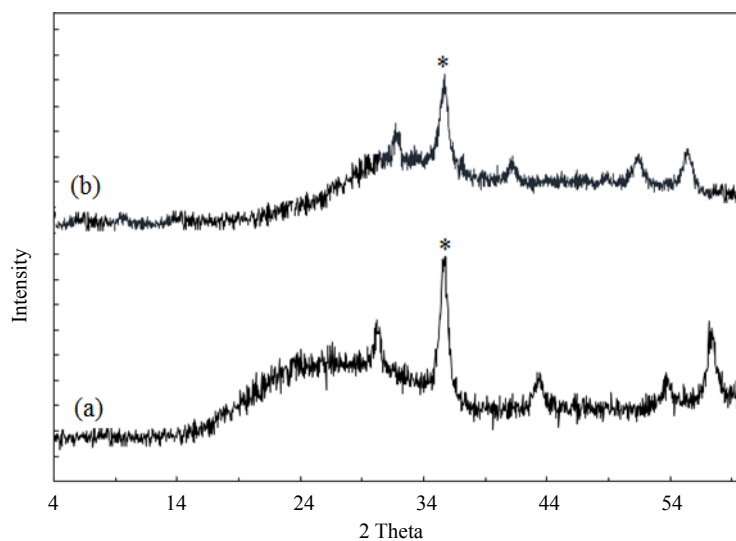


Fig. 3: XRD patterns for Fe_3O_4 (a) and drug loaded $\text{Fe}_3\text{O}_4@\text{SiO}_2\text{-NH}_2$ (b).

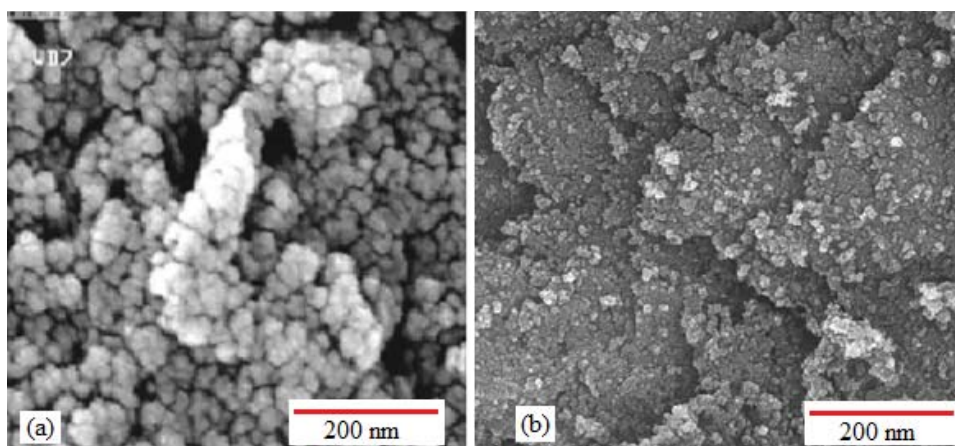


Fig. 4: FESEM image and size distribution of the Fe_3O_4 (a) and $\text{Fe}_3\text{O}_4@\text{SiO}_2\text{-NH}_2$ (b) nanoparticles.

Loading/release studies

Considering the influence of hydrogen bonding on the loading of the drug onto the pores of the modified nanomagnetic material, further studies were outlined to clarify loading and release efficacies. Main parameters on the acyclovir loading seem to be pH, loading time and temperature.

The impact of pH on the loading of acyclovir was performed at various pHs, ranging from acidic to basic. As Fig. 5 shows, the best loading can be achieved at pH 9. This loading pattern can be assigned to the increments of the hydrogenic interactions in an alkaline pH. The decrease in

loading was observed at high alkaline pHs (>10) merely due to the hydrolysis of Fe–O–Si and C–O–Si bands and demolition of the grafted agent. The loading temperature was also screened on the drug loading capacity. Findings displayed that by enhancing temperature, the drug loading improves. This phenomenon can be attributed to decreasing of desorption because of the hydrogenic interactions by raising temperature [30]. Effect of time on the loading of acyclovir onto $\text{Fe}_3\text{O}_4@\text{SiO}_2\text{-NH}_2$ was also investigated. As Fig. 6 shows, the loading time of 5 h was selected as the optimum. Considering the important role of temperature on the loading of the drug and considering the body

temperature, three different temperatures 37, 45, and 55 °C were investigated (Fig. 7). Results showed that by increasing temperature, the drug loading was increased and the best loading achieved at 55 °C. Release of the drug was also studied as a main parameter affecting efficiency

of the introduced drug carrier system. The two important parameters of pH and release time were investigated (Figs. 8-9). Outcomes showed that there was no acyclovir leak at pH 9; whereas by decreasing pH to 5, hydrogen bonding would be diminished and acyclovir was released gradually.

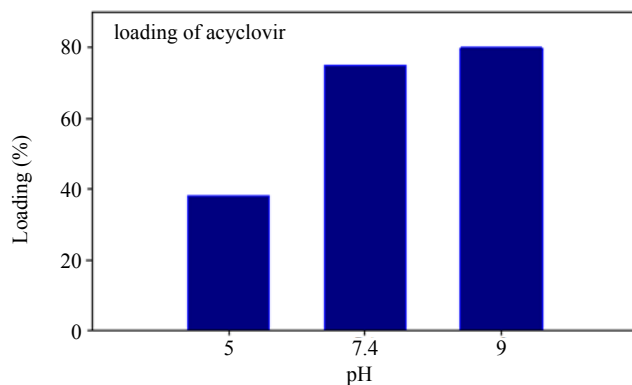


Fig. 5: Effect of pH on loading of acyclovir onto Fe₃O₄@SiO₂-NH₂.

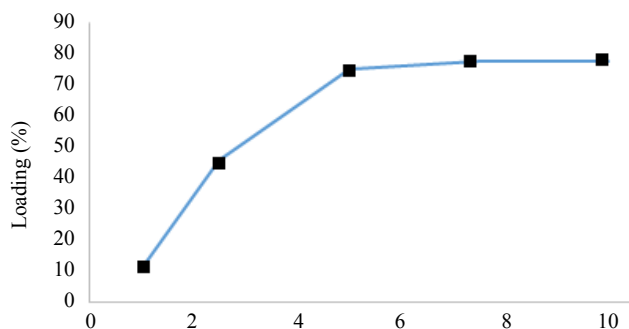


Fig. 6: Effect of contact time on loading of acyclovir onto Fe₃O₄@SiO₂-NH₂.

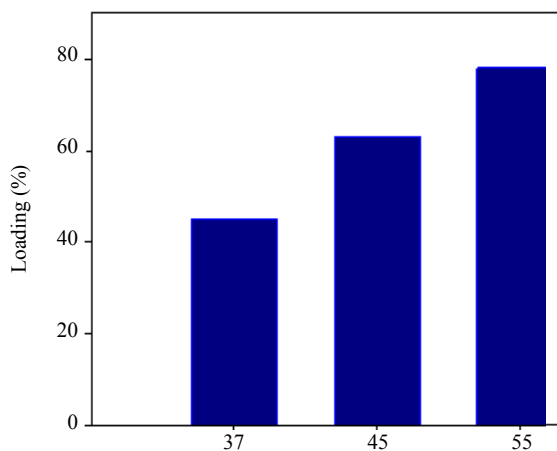


Fig. 7: Effect of temperature on loading of acyclovir onto Fe₃O₄@SiO₂-NH₂.

Therefore, it can be concluded that loading and release of acyclovir from $\text{Fe}_3\text{O}_4@\text{SiO}_2\text{-NH}_2$ can be controlled by pH. Therefore, this material would be an impressive carrier for oral acyclovir delivery. Eventually, the release time was monitored (Fig. 8). The slow release of acyclovir reached to 78% in 48 h which is another benefit for this drug carrier system. This slow release rate would be attributed to the strong interactions of the surface amine groups of the carrier with acyclovir.

Among several parameters which should be optimized in order to obtain maximum adsorption capacity and slow drug release, effect of amine functionalization on the drug carrier efficiency was compared with the results obtained from the unmodified Fe_3O_4 and $\text{Fe}_3\text{O}_4@\text{SiO}_2$ nanoparticles. As Table 1 shows, functionalization has been essential to attain acceptable loading capacity and suitable release time under the selected pH and temperature.

Table 1 Effect of functionalization with silanol and amine groups on the delivery of acyclovir.

Carrier	Drug loading (%)	Loading time (h)	Release (%)	Release time (h)
Fe_3O_4	9	5	not determined	
$\text{Fe}_3\text{O}_4@\text{SiO}_2$	44	5	76 (in pH 7.4)	48
$\text{Fe}_3\text{O}_4@\text{SiO}_2\text{-NH}_2$	78	5	72 (in pH 7.4) 77 (in pH 5) 84 (in pH 9)	48

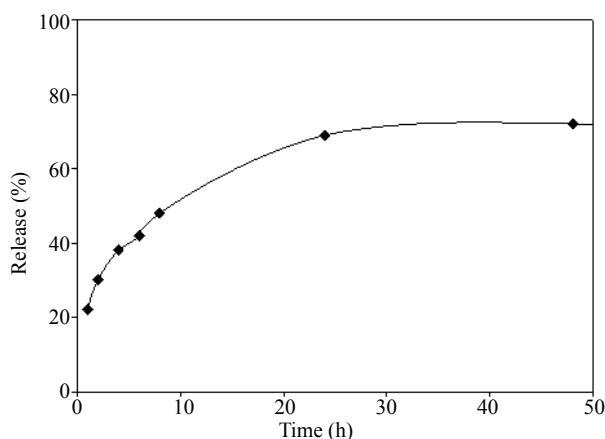


Fig. 8: Effect of time on the release of acyclovir from $\text{Fe}_3\text{O}_4@\text{SiO}_2\text{-NH}_2$.

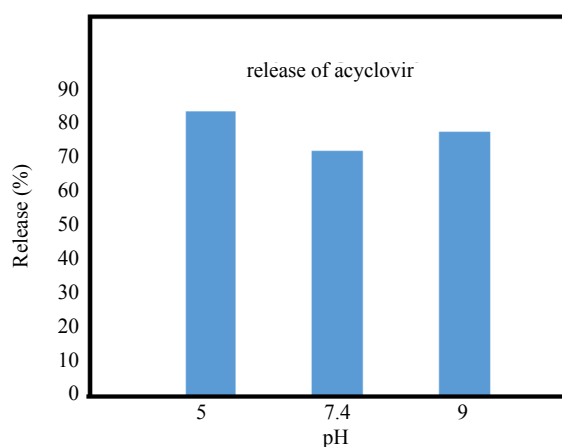


Fig. 9: Effect of pH on the release of acyclovir from amine functionalized $\text{Fe}_3\text{O}_4@\text{SiO}_2\text{-NH}_2$.

CONCLUSION

In summary, the uniform Fe₃O₄ nanoparticles were successfully synthesized through the solvothermal method. Then, the prepared nanoparticles were enriched with silanol groups and were finally modified with TMPA to improve their efficiencies in the delivery of acyclovir. The introduced biocompatible delivery system showed very good capacity for storage of a large amount of acyclovir. In addition to the high loading capacity, the modified nanoporous material released the drug in a long period, especially independent to pH. In order to show the necessity of modification, the efficiency of the amine-modified nanomaterial was compared with Fe₃O₄ and Fe₃O₄@SiO₂ and the results demonstrated that modification has been absolutely effective.

ACKNOWLEDGMENTS

Partial financial support from the Research Councils of Sabzevar University of Medical Sciences and Hakim Sabzevari University is greatly appreciated.

CONFLICT OF INTEREST

The authors declare that there is no conflict of interests regarding the publication of this manuscript.

REFERENCES

- [1] Knop K., Hoogenboom R., Fischer D., Schubert U. S., (2010), Poly (Ethylene Glycol) in drug delivery: Pros and cons as well as potential alternatives. *Angew. Chem. Int. Ed. Eng.* 49: 6288-6295.
- [2] Peer D., Karp J. M., Hong S., Farokhzad O. C., Margalit R., Langer R., (2007), Nanocarriers as an emerging platform for cancer therapy. *Nat. Nanotechnol.* 2: 751-758.
- [3] Shi J., Votrubka A. R., Farokhzad O. C., Langer R., (2010), Nanotechnology in drug delivery and tissue engineering: From discovery to applications. *Nano Lett.* 10: 3223-3229.
- [4] Dreaden E. C., Alkilany A. M., Huang X., Murphy C. J., (2012), The golden age: Gold nanoparticles for biomedicine. *Chem. Soc. Rev.* 41: 2740-2747.
- [5] Torchilin V. P., Lukyanov A. N., (2003), Peptide and protein drug delivery to and into tumors: Challenges and solutions. *Drug. Discov. Today.* 8: 259-267.
- [6] Bae Y., Kataoka K., (2009), Intelligent polymeric micelles from functional poly (ethylene glycol)-poly (amino acid) block copolymers. *Adv. Drug. Deliv. Rev.* 61: 768-776.
- [7] Kaasgaard T., Andresen T. L., (2010), Liposomal cancer therapy: Exploiting tumor characteristics. *Expert. Opin. Drug. Deliv.* 7: 225-234.
- [8] Astruc D., Boisselier E., Ornelas C., (2010), Dendrimers designed for functions: from physical, photophysical and supramolecular properties to applications in sensing, catalysis, molecular electronics, photonics and nanomedicine. *Chem. Rev.* 110: 1857-1863.
- [9] Thakor A. S., Jokerst J., Zavaleta C., Massoud T. F., Gambhir S. S., (2011), Gold nanoparticles: A revival in precious metal administration to patients. *Nano Lett.* 11: 4029-4038.
- [10] Hammond P. T., (2004), Form and function in multilayer assembly: New applications at the nanoscale. *Adv. Mater.* 16: 1271-1278.
- [11] Ginebra M. P., Traykova T., Planell J. A., (2006), Calcium phosphate cements as bone drug delivery systems: A review. *J. Control. Rel.* 113: 102-107.
- [12] Patri A. K., Majoros L. J., Baker J. R., (2002), Dendritic polymer macromolecular carriers for drug delivery. *Curr. Opin. Chem. Bio.* 16: 466-473.
- [13] Rezwani K., Chen Q. Z., Blaker J. J., Boccaccini A. R., (2006), Biodegradable and bioactive porous polymer/inorganic composite scaffolds for bone tissue engineering. *Biomaterials* 27: 3413-3418.
- [14] Horcajada P., Chalati T., Serre C., Gillet B., Sebrie C., (2010), Porous metal-organic-framework nanoscale carriers as a potential platform for drug delivery and imaging. *Nat. Mater.* 9: 172-178.
- [15] Zahir Abadi I. J., Sadeghi O., Lotfzadeh H. R., Tavassoli N., Amini V., Amini M. M., (2012), Novel modified nanoporous silica for oral drug delivery: Loading and release of clarithromycin. *J. Sol Gel Sci. Technol.* 61: 90-95.
- [16] Tang F., Li L., Chen D., (2012), Mesoporous silica nanoparticles: Synthesis, biocompatibility and drug delivery. *Adv. Mater.* 24: 150-156.
- [17] Tang Q., Xu Y., Wu D., Sun Y., Wang J., (2006), Studies on a new carrier of trimethylsilyl-modified mesoporous material for controlled drug delivery. *Control. Rel.* 114: 41-46.
- [18] Trewyn B. G., Giri S., Slowing I. I., Lin V. S. Y., (2007), Mesoporous silica nanoparticle based controlled release, drug delivery and biosensor systems. *Chem. Commun.* 31: 3236-3241.
- [19] Yang Q., Wang S. H., Fan P., Wang L., Di Y., Lin K., Xiao F. S., (2005), pH-responsive carrier system based on carboxylic acid modified mesoporous silica and polyelectrolyte for drug delivery. *Chem. Mater.* 17: 59-68.
- [20] Chomchoey N., Bhongsuwan D., Bhongsuwan T., (2010), Magnetic properties of magnetite nanoparticles synthesized by oxidative alkaline hydrolysis of iron powder. *J. Nat. Sci.* 44: 963-971.
- [21] Hoa L. T. M., Dung T. T., Danh T. M., Duc N. H., Chien D. M., (2009), Preparation and characterization of magnetic nanoparticles coated with polyethylene glycol. *J. Phys.* 187: 12-18.
- [22] Acar H. Y. C., Garaas R. S., Syud F., Bonitatebus P., Kulkarni A. M., (2005), Superparamagnetic nanoparticles stabilized by polymerized PEGylated coatings. *J. Magn. Magn. Mater.* 293: 1-8.
- [23] Huang Y., Zhang L., Huan W., Xiaojuan L., Yang Y., (2010), A study on synthesis and properties of Fe₃O₄ nanoparticles by solvothermal method. *Glass Phys. Chem.* 36: 325-331.
- [24] Saadatjoo N., Golshekana M., (2013), Organic/inorganic MCM-41 magnetite nanocomposite as a solid acid catalyst for synthesis of benzo [α] xanthenone derivatives. *J. Mol. Catal. A: Chem.* 377: 173-179.
- [25] Maniya N. H., Sanjaykumar R. P., Murthy Z. V. P., (2015), Controlled delivery of acyclovir from porous silicon micro- and nanoparticles. *Appl. Sur. Sci.* 330: 358-363.
- [26] Huang S. T., Du Y. Z., (2001), Synthesis and anti-hepatitis B virus activity of acyclovir conjugated stearic acid-g-chitosan oligosaccharide micelle. *Carbohydr. Polym.* 83: 1715-1722.
- [27] Liu X., Ma Z., Xing J., Liu H., (2004), Preparation and characterization of amino-silane modified superparamagnetic silica nanospheres. *J. Magn. Magn. Mater.* 270: 1-8.
- [28] Masteri-Farahani M., Tayyebi N., (2011), A new magnetically recoverable nanocatalyst for epoxidation of olefins. *J. Mol. Catal. A: Chem.* 348: 83-88.
- [29] Banerjee S. S., Chen D. H., (2007), Magnetic nanoparticles grafted with cyclodextrin for hydrophobic drug delivery. *Chem. Mater.* 19: 6345-6349.
- [30] Moazzen E., Ebrahimzadeh H., Amini M., Sadeghi O., (2013), A novel biocompatible drug carrier for oral delivery and controlled release of antibiotic drug: loading and release of clarithromycin as an antibiotic drug model. *J. Sol. Gel Sci. Technol.* 66: 345-352.